EXTREME-RELATIVISTIC CROSS SECTIONS FOR COMPTON SCATTERING BY K-SHELL ELECTRONS

V. Florescu[1] and M. Gavrila[2]
[1]Department of Physics, University of Bucharest, Bucharest-Magurele MG11, 76900, Romania
[2]Institute for Theoretical Atomic and Molecular Physics, Harvard-Smithsonian Center for Astrophysics, Cambridge, MA 02138

November 25, 2002

Abstract

We report on progress of our project on extreme relativistic (ER) Compton scattering of very hard incident photons $\left(\hbar\omega_1 \gg mc^2\right)$ from bound electrons. We have considered the case of a Coulomb atomic potential, of arbitrary nuclear charge Z. The calculation of the ER form of the S-matrix element was done with an analytical method. In the present case, this is a viable alternative to an impracticable *ab initio* numerical computation. In order to obtain the dominant behavior of the matrix element in the large ω_1 limit, the momentum transferred to the nucleus Δ need be ascribed a constant (albeit arbitrary) value in the limiting process. The result depends critically on the spectral range in which the scattered-photon energy ω_2 is situated. We have considered the ω_2 range covering the Compton line, for which the ratio ω_2/ω_1 need be kept finite. The triply differential cross section, $d^3\sigma_{ER} \,/\, d\omega_2 d\Omega_2 d\Delta$, was calculated for the range of Compton line in terms of hypergeometric Appell functions. This is a rather unique example of a most elaborate Coulomb problem that could be solved analitically, in closed form. Finally, we report numerical results for the triply differential cross section, that has attracted theoretical and experimental interest recently.

1 Introduction

An extensive theoretical and experimental effort has been invested in the study of Compton scattering by bound electrons, for photon energies ranging from keV's to about 1 MeV. Specific of the bound-electron Compton effect, in comparison to its free electron counterpart, is the width acquired by the line and its shifted position. For references, see the book by Williams [1], concerning the lower (nonrelativistic) energy photon range, and for the higher (relativistic) range, the review article by Bergstrom and Pratt [2], and a special issue of *Radiation Physics and Chemmistry* [3].

The most significant theoretical advancement in the relativistic energy range in the last decade was the "numerical S-matrix approach", developed by Suric, Bergstrom, Pisk, and Pratt [4], [5]. Their program is capable of handling all atomic shells, within the independent-electron approximation with a relativistic central potential of the Hartree-Fock-Slater type. It is limited, however, at high incoming photon energies $\hbar\omega_1$ by the convergence of the partial wave summations it is based on; in practice, this limitation sets in at about $\hbar\omega_1 \simeq 2mc^2$.

We have been considering recently the problem of Compton scattering by K-shell electrons in the *extreme relativistic (ER) limit*, i.e., for incident photons $\hbar\omega_1 >> mc^2$, in order to cover the photon range left open by the numerical S-matrix approach. We have treated the case of a Coulomb potential of arbitrary Z, and have integrated the S-matrix element in the Furry picture of QED. Our only approximation was to retain consistently the dominant order in $mc^2 / \hbar\omega_1$. We note that the ER limit of bound-electron Compton scattering was analyzed by Pauli and Heisenberg (see [7]), early on in the development of relativistic quantum mechanics, although no cross section was obtained.

The method we use for integrating the ER matrix element is based on a combination of analytic procedures that we have developed earlier in related contexts (NR Compton scattering, Gavrila [8], [9], and ER Rayleigh scattering, Florescu and Gavrila [10]). We have shown that the Dirac spinors and Green's operator needed in the calculation of the *extreme relativistic* Compton matrix element can be replaced by their *nonrelativistic* counterparts, taken with relativistically modified parameters. This has allowed the integration of the ER matrix element in a manner similar to the NR case [8]. We have here a most elaborate Coulomb problem for which it was possible to complete the calculation analytically and obtain the result in closed form (hypergeometric functions), in a situation when a direct numerical computation is still prohibitive. Our analytic result is part of an ongoing project on the study of ER Compton scattering. Within the same project, we have presented earlier the discussion of the infrared problem associated with the ER scattering [6].

Beside a brief presentation of our analytic results, we shall also give a numerical application, namely the computation of the Compton cross section triply differential with respect to the scattered photon energy and angles, and to the angles of ejected electron (expressed in terms of the total momentum transfer to the nucleus Δ), $d^3\sigma_{ER} / d\kappa_2 \, d\Omega_2 \, d\Delta$. This cross section is an intermediate step in our project, aimed at the computation of $d^2\sigma_{ER} \; / \, d\kappa_2 \, d\Omega_2$. We note that, recently, Kaliman, Suric, Pisk and Pratt [13] have calculated the triply differential cross section within the numerical S-matrix approach, for Cu and Pb at several incident energies (the highest of which was 662 keV), motivated by experimental research (see [13], for references). As in the case of the doubly differential cross-section, such numerical calculations become prohibitive at higher photon energies, and alternative methods are needed.

Our endeavor was encouraged by the new developments in the production of laboratory hard photons. γ-ray photons with energies as high as 32 MeV have been reported, and energies up to some 225 MeV are considered to be attainable (see [11]). With all the progress achieved in terrestrial labs, however, there is no way that these can compete with cosmic γ-ray sources, since photons of up to 10^7 MeV have been observed to be emitted from the center of "active galaxies" (see [12]).

The content of the paper is the following. The physics of the high-energy limit of the Compton effect is presented Sec.II. Our analytic calculation of the cross sections is outlined in Sec.III. Finally, in Sec.IV we present the numerical results for the triple differential cross-section.

2 ER matrix elements and cross sections

In the initial state of the process, we are dealing with a bound K-shell electron of energy $E_0 \equiv \gamma = \left(1-a^2\right)^{1/2}$ and magnetic quantum number m_1, plus a photon of momentum $\boldsymbol{\kappa_1}$, energy $\omega_1 \equiv \kappa_1$, and polarization vector $\mathbf{s_1}$. In the final state we have a continuum electron of asymptotic momentum $\mathbf{p}$, energy $E_p = \left(1+p^2\right)^{1/2}$, and magnetic quantum number m_2, the scattered photon having momentum $\boldsymbol{\kappa_2}$, energy $\omega_2 \equiv \kappa_2$, and polarization vector $\mathbf{s_2}$. We are using natural units $(\hbar = m = c = 1)$, and denote $a \equiv \alpha Z$, where α is the fine structure constant (in natural units $\alpha = e^2$).

The *quadruply differential cross section* for the Compton effect, in which all characteristics of the particles involved are recorded, can be written as

$$d^4\sigma = \alpha^2 \frac{\kappa_2}{\kappa_1} \left|M^{(C)}\right|^2 \delta\left(E_0 + \kappa_1 - E_p - \kappa_2\right) p^2 dp d\Omega_p d\kappa_2 d\Omega_2 \; , \qquad (1)$$

where $d\Omega_2$ refers to the angles of $\boldsymbol{\kappa_2}$, and the δ function takes care of the conservation of energy

$$E_0 + \kappa_1 = E_p + \kappa_2 \; . \qquad (2)$$

The matrix element entering here is given by

$$M^{(C)} = M^{(1)} + M^{(2)} \, , \qquad (3)$$

where $M^{(1)}$ is the term corresponding to the Furry diagram "absorption first":

$$\begin{aligned} M^{(1)} &= \int\!\!\int u^{(-)\dagger}_{\mathbf{p}m_2}\left(\mathbf{r_2}\right) e^{-i\boldsymbol{\kappa_2}\cdot\mathbf{r_2}} \\ &\times \left(\boldsymbol{\alpha}\cdot\mathbf{s_2}\right) G\left(\mathbf{r_2},\mathbf{r_1};\Omega_1\right)\left(\boldsymbol{\alpha}\cdot\mathbf{s_1}\right) e^{i\boldsymbol{\kappa_1}\cdot\mathbf{r_1}} u_{om_1}\left(\mathbf{r_1}\right) \mathbf{dr_1 dr_2} \, , \end{aligned} \qquad (4)$$

A similar formula can be written for $M^{(2)}$ describing the diagram "emission first". $u_{om_1}\left(\mathbf{r_1}\right)$ is the initial spinor of the electron, $u^{(-)}_{\mathbf{p}m_2}\left(\mathbf{r_2}\right)$ is the final, continuum spinor with incoming asymptotic spherical waves, normalized per momentum interval, and $\boldsymbol{\alpha}$ the Dirac matrices. $G\left(\mathbf{r_2},\mathbf{r_1};\Omega\right)$ is the Green's function for the Dirac equation, with energy parameter Ω. Ω_1 in Eq.(4) is given by

$$\Omega_1 = E_0 + \kappa_1 + i\epsilon \, , \qquad \epsilon \to 0^+ \, . \qquad (5)$$

In the following, we shall not be interested in the dependence of the cross section on all the characteristics of the photons and electrons. We shall consider initially polarized photons but will not analyze their final polarizations. Neither shall we analyze the final polarizations of the electron. The corresponding quadruply differential cross section per K-shell electron is

$$\begin{aligned} d^4\widetilde{\sigma} &= \alpha^2 \frac{\kappa_2}{\kappa_1} \\ &\times \sum_{\mathbf{s_2}} \frac{1}{2} \sum_{m_1,m_2} \left|M^{(C)}\right|^2 \delta\left(E_0 + \kappa_1 - E_p - \kappa_2\right) p^2 dp \, d\Omega_p \, d\kappa_2 d\Omega_2 \; . \end{aligned} \qquad (6)$$

The goal of our work is to extract the dominant behavior, exact in Z, of the matrix element Eq.(3) and cross section Eqs.(6), for $\kappa_1 \to \infty$. We have shown that this is obtained by keeping the momentum transferred to the nucleus,

$$\mathbf{\Delta} \equiv \boldsymbol{\kappa_2} - \boldsymbol{\kappa_1} - \mathbf{p}\,, \tag{7}$$

constant in the process. Our ER limit is thus characterized by the conditions:

$$\kappa_1 \to \infty, \quad \Delta = finite\;. \tag{8}$$

The ER calculation of the matrix element and cross sections depends on the range of the scattered photon spectrum considered. One can distinguish three main ranges:

(i) The *soft-photon end,* defined by

$$\kappa_2 < \epsilon, \tag{9}$$

where $\epsilon > 0$ and sufficiently small. We have found that $\mathbf{p}$ and $\boldsymbol{\kappa_1}$ are quasi-parallel. Moreover, in this range, the Compton effect and photoeffect are connected theoretically by the "soft-photon theorem". This case was discussed in detail in [6].

(ii) The *Compton-line,* defined by $\eta \equiv (\kappa_2/\kappa_1)$ = const, with η such that

$$\epsilon' < \eta < 1 - \varpi\,; \tag{10}$$

here ϵ' , $\varpi > 0$ are nonzero, sufficiently small quantities. Again, $\mathbf{p}$ and $\boldsymbol{\kappa_1}$ are quasi-parallel; $p \to \infty$

(iii) The *tip of the spectrum,* located in the vicinity of $\kappa_2^{\max} = E_0 + \kappa_1 - 1$, hence having $p \cong 0$. In this vicinity, $\kappa_2 \cong \kappa_1 \to \infty$, but $\eta < 1$ (strictly).

Important kinematic conclusions for the range of the Compton line can be drawn by manipulating the energy conservation equation Eq.(2) when expressed in terms of $\mathbf{\Delta}$ rather than $\mathbf{p}$. These are:

(1) The quantity

$$\xi \equiv \kappa_1 \left(1 - \boldsymbol{\nu_1} \cdot \boldsymbol{\nu_2}\right) = 2\kappa_1 \sin^2 \frac{\theta}{2}\;, \tag{11}$$

where $\boldsymbol{\nu_i} \equiv \boldsymbol{\kappa_i}/\kappa_i$ (i=1,2) and θ is the angle between them, needs to be kept constant (albeit arbitrary) in the ER limit. This implies that the relevant scattering occurs at infinitesimal angle θ as κ_1 increases; therefore: $\xi \simeq \kappa_1 \left(\theta^2/2\right)$. We note that already Heisenberg and Pauli [7, Sec.1], had realized that Eqs.(8), (10), and ξ =const, were the key conditions needed to define the ER limit, although no proof was given.

(2) The angle of $\mathbf{\Delta}$ with $\boldsymbol{\nu_1}$ is fixed, such that its cosine, w, is given by

$$w = \frac{q}{\Delta}\;, \; where \quad q \equiv \frac{\eta}{(1-\eta)}\xi - \gamma\;. \tag{12}$$

(3) Δ is limited by

$$\Delta \;\geq\; |q|\;. \tag{13}$$

With this in mind, the quadruply differential cross section can be written (at $\xi \neq 0$)

$$\frac{d^4\widetilde{\sigma}_{ER}}{d\kappa_2 d\Omega_2\, d\Delta d\Phi} = \alpha^2\, \eta\; \Delta \sum_{\mathbf{s}_2} \frac{1}{2} \sum_{m_1, m_2} \left| \widetilde{M}^{(C)}_{ER} \right|^2 . \tag{14}$$

Here $\widetilde{M}^{(C)}_{ER}$ is the ER form of the matrix element Eq.(3), with w fixed by Eq.(12); Φ is the azimuthal angle around $\boldsymbol{\Delta}$. We shall be interested in the following in the cross section $d^3\sigma_{\,ER}\,/d\kappa_2 d\Omega_2\, d\Delta$, obtained by integrating Eq.(14) over Φ. By integrating further over Δ , one obtains the doubly differential cross section $d^2\sigma_{\,ER}/\,d\kappa_2 d\Omega_2$, to be discussed elsewhere.

3 Analytic calculation of matrix elements and cross sections

The *method of integration* we use for the ER matrix element of the Compton-line range [case *(ii)*] is a combination of procedures applied earlier in similar contexts (NR Compton scattering, Gavrila [8], [9]; ER Rayleigh scattering, Florescu and Gavrila [10]). The matrix element $M^{(C)}$ is integrated in momentum space. For the final continuum spinor of the electron we use a high-energy approximation (recall that $p \to \infty$), equivalent to the Sommerfeld-Maue approximation (for the latter see, e.g., [15, Sec.5.8]; [14]). Its essential ingredient is the NR Schrödinger continuum wave function, with relativistically modified parameters. This is described by an integral representation. For the relativistic Green's function of the problem we also use a high-energy approximation (note that $\Omega_1 \to \infty$ in the ER limit) equivalent to the corresponding Sommerfeld-Maue approximation (for the latter, see Hostler [17]). Here, the essential ingredient is the NR Green's function with relativistically modified parameters, for which we use the integral representation of Schwinger [16] and Hostler [18] in momentum space. The relativistic K-shell electron is described exactly, using an integral representation involving the NR $1s$ wave function. Thus, the ingredients used in the calculation of the *extreme-relativistic* matrix element turn out to be reducible to their *nonrelativistic* counterparts taken, however, with relativistically modified parameters. At start, the matrix element $M^{(C)}$ appears thus as a succession of 6 momentum integrals (from the original matrix element), followed by three integral representations, a total of nine integrals. The ER limit of the integrand is then taken, as was done in [10], which simplifies its expression. In this manner, the integration of the relativistic matrix element becomes similar to that of the NR one, see [8]. The momentum integrations are carried out exactly by a technique developed by Gavrila and Costescu [19]. The integral representations of the final spinor and of the Green's function can also be carried out exactly (application of residue theorem in the first case, and, in the second case, quite remarkably, by finding the primitive of the integrand). Thereby, $M^{(C)}$ is expressed in terms of a single parametric integral. This integral can be expressed further in terms of hypergeometric functions of two variables, of the Appell type $F_1\,(a; b_1, b_2; c; x_1, x_2)$, defined in [20, Sec.5.8.2]. At the end, we are left to carry out the tedious summations over the electron and photon polarizations appearing in the cross section Eq.(14).

Finally, the quadruply differential cross section Eq.(14) can be written at

$\xi \neq 0$ as

$$\frac{d^4\widetilde{\sigma}_{ER}}{d\kappa_2 d\Omega_2 d\Delta d\Phi} = \alpha^2 \, \frac{1}{\kappa_1} \frac{\left(1+\eta^2\right)}{\eta\,\xi} \; T\,\Delta\,. \tag{15}$$

We have defined here

$$T = |K|^2 \, \left\{ |2\,(L_1 + L_2)|^2 + \left(1 - \frac{q^2}{\Delta^2}\right) |\,L_3|^2 \right\} \,, \tag{16}$$

where

$$\begin{aligned} L_1 &= \frac{2}{\left(\Delta^2 + a^2\right)^2} \, \frac{1 - ia}{3 - ia} \,, \\ &\quad \times \left[(1 + \gamma + q)\,(2 + \gamma - ia)\; u^{\gamma-1}\, F^{(2)} + a^2\, u^{\gamma-2}\, F^{(3)} \right] , && (17) \\ L_2 &= \frac{(1 + \gamma + ia)}{(\Delta^2 + a^2)\,(q - ia)} \;\; u^{\gamma-1} F^{(1)}, && (18) \\ L_3 &= -\,\frac{4\Delta}{\left(\Delta^2 + a^2\right)^2} \, \frac{1 - ia}{3 - ia} \; (2 + \gamma - ia)\; u^{\gamma-1}\, F^{(2)}, && (19) \\ |K|^2 &= \frac{a^5}{16\pi^2} \, \frac{2^{2\gamma}}{(1+\gamma)\Gamma(1+2\gamma)} \left(\frac{2\pi a}{1 - e^{-2\pi a}}\right) \left| \frac{\Gamma(2 + \gamma - ia)}{\Gamma(3 - ia)} \right|^2 e^{2a\Psi_1} . && (20) \end{aligned}$$

We have further denoted

$$u \equiv \frac{ia}{ia - q} \;\;, \tag{21}$$

$$\begin{aligned} F^{(1)} &\equiv F_1\,(1-\gamma; 1 - ia, 1 - ia; 3 - ia;\; z_+\,,\; z_-)\,, && (22) \\ F^{(2)} &\equiv F_1\,(1-\gamma; 2 - ia, 2 - ia; 4 - ia;\; z_+\,,\; z_-)\,, && (23) \\ F^{(3)} &\equiv F_1\,(2-\gamma; 2 - ia, 2 - ia; 4 - ia;\; z_+\,,\; z_-)\,, && (24) \end{aligned}$$

with

$$z_+ \equiv \frac{\Delta\, +\, q}{\Delta\, +\, ia} \;\;, \quad z_- \equiv \frac{\Delta\, -\, q}{\Delta\, -\, ia} \;\;, \tag{25}$$

and

$$\tan\Psi_1 = -\,(a\,/\,q) \;\;,\;\; -\pi \leq \Psi_1 \leq 0\;. \tag{26}$$

We note that there is no $\mathbf{s}_1$ dependence left in the expression of the cross-section (15).

As the right hand side in Eq.(15) does not depend on Φ, one may immediately write the *ER triply differential cross section* at $\xi \neq 0$ as

$$\frac{d^3\sigma_{ER}}{d\kappa_2 d\Omega_2 d\Delta} = \alpha^2 \; \frac{2\pi}{\kappa_1} \frac{\left(1+\eta^2\right)}{\eta\,\xi} \; T\;\Delta\;, \tag{27}$$

and the *ER doubly differential cross section* as

$$\frac{d^2\sigma_{ER}}{d\kappa_2 d\Omega_2} = 2\pi\,\alpha^2 \frac{1}{\kappa_1} \frac{\left(1+\eta^2\right)}{\eta\,\xi} \; \int_{|q|}^{\infty} T\Delta\, d\Delta\,. \tag{28}$$

Note that the integral over Δ is a function of a and q, and that ξ and η are contained only in q of Eq.(12). The evaluation of the Appell functions involved, as well as the integration over Δ, has to be carried out numerically.

4 Computation of triply differential cross section

The quantity we have evaluated numerically is

$$\Sigma_R\,(Z,\xi,\eta\,;\Delta) \equiv \kappa_1\,\frac{d^3\sigma_R}{d\kappa_2\,d\Omega_2\,d\Delta}\,. \tag{29}$$

This, we shall consider as a function of Δ, depending parametrically on ξ, η, and Z. Consequently, the area under the curve $\Sigma_R\,(Z,\xi,\eta\,;\Delta)\;/\;\kappa_1$ gives the doubly differential cross section, Eq.(28). At given ξ, the latter gives the spectral distribution of the Compton line (variable η), whereas at constant η, it gives its angular distribution (variable ξ). As known, both distributions peak in the vicinity of the Compton line for a free electron, which we shall denote by ξ_0 and η_0, respectively. These are related by the Compton equation, which in the ER limit reads

$$\frac{\xi_0\,\eta_0}{(1-\eta_0)} = 1\,. \tag{30}$$

We have chosen in the following to represent $\Sigma_R\,(Z,\xi,\eta\,;\Delta)$ for pairs of parameters (ξ,η) in the vicinity of (ξ_0,η_0).

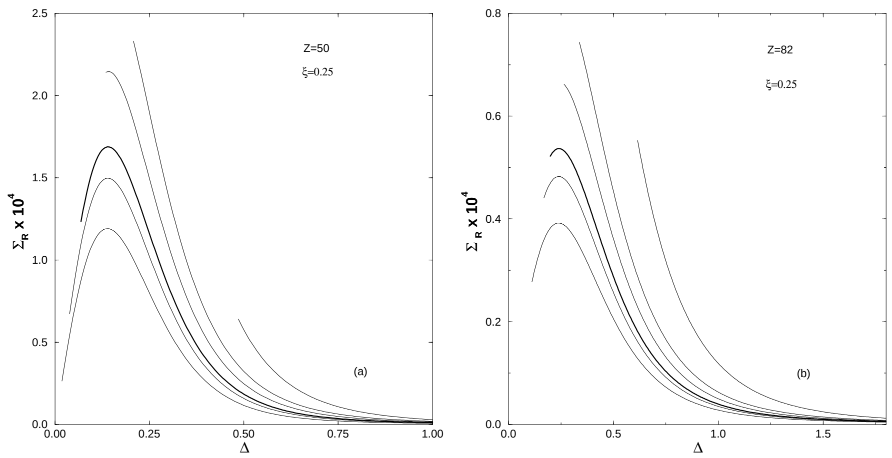

Fig.1 Triply differential cross-section Σ_R, Eq.(29), in natural units, as function of Δ, in natural units,, $\xi = 0.25$ and different values of η, from bottom to top: 0.785, 0.795, 0.800, 0.810, 0.820 and 0.850. The thick solid line at $\eta = 0.800$ corresponds to the free electron Compton line. (a) $Z = 50$. (b) $Z = 82$.

In Figs.1 (a) and (b) we give Σ_R at $\xi = 0.25$, for $Z = 50$ and 82, respectively, at η as indicated. The corresponding value of η_0 for the free electron Compton peak is 0.8; the associated curves for Σ_R are represented by thick solid lines. As apparent, the curves for Σ_R do not start at the same value of Δ. This is because Δ has physical meaning only if Eq.(13) is satisfied. In the cases shown, the minimal value of $\Delta_m = |q|$ moves to the right as η increases. This, however, is not the case at low Z. One notices that, as Δ_m increases, it cuts through the maximum of Σ_R, reducing Σ_R eventually to only its descending branch.

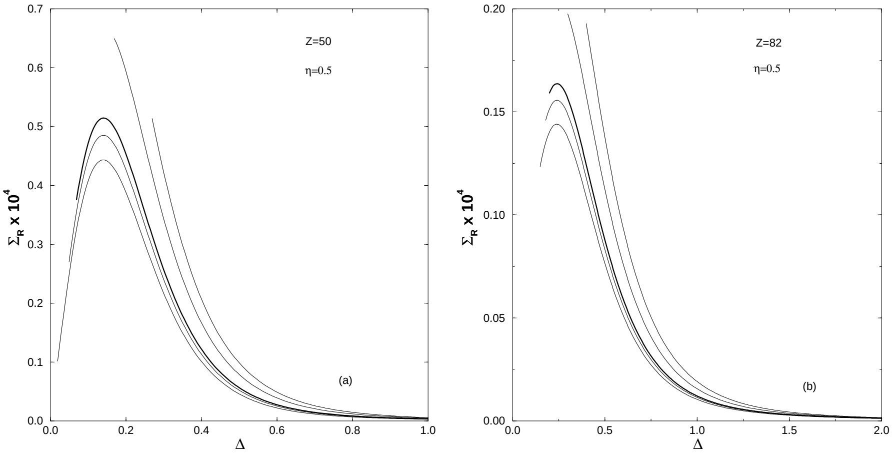

Fig.2 Triply differential cross-section Σ_R, Eq.(29), in natural units, as function of Δ, in natural units, $\eta = 0.5$ and different values of ξ, from bottom to top: 0.950, 0.980, 1.00, 1.10, 1.20 The thick solid line at $\xi = 1.00$ corresponds to the free electron Compton line. (a) $Z = 50$. (b) $Z = 82$.

In Figs. 2 (a) and 2 (b) we give Σ_R at $\eta = 0.5$, for $Z = 50$ and 82, respectively, at ξ as indicated. A similar representation as in Figs. 1 and 2 was adopted. The corresponding value of ξ_0 for the free electron Compton peak is 1.

With decreasing Z the triply differential cross-section becomes narrower. In the limit $Z \to 0$ the distribution has the behaviour of $\delta(\Delta)$, as should be, because for a free particle momentum is conserved. This can be checked also analytically.

The calculation of the triply differential cross section described here, will allow us to pass to that of the doubly differential one, $d^2\sigma_{ER} \,/\, d\kappa_2\, d\Omega_2$, closely related to the Klein-Nishina cross section for the free electron.

5 Aknowledgments

The authors are indebted to Richard H. Pratt for a fruitful collaboration extending over four decades. They would also like to thank Alex Dalgarno for his hospitality at ITAMP, where much of this work was done.

References

[1] B. Williams, *Compton Scattering* (McGraw-Hill, 1977).

[2] P.M. Bergstrom and R.H. Pratt, Radiat.Phys.Chem. **50** , 3 (1997).

[3] Rad.Phys.Chem.**50**, No. 1, July 1997, dedicated to *Inelastic Scattering of X-rays and γ-rays.*

[4] T. Suric, P.M. Bergstrom Jr, K. Pisk, and R.H. Pratt, Phys.Rev.Lett. **67**, 189 (1991).

[5] P.M. Bergstrom Jr, T. Suric, K. Pisk, and R.H. Pratt, Phys.Rev.A **48**, 1134 (1993).

[6] V. Florescu and M. Gavrila, Radiat.Phys.Chem. **59**, 127 (2000).

[7] W. Pauli, Helv.Phys.Acta **6**, 279 (1933).

[8] M. Gavrila, Phys.Rev.A **6**, 1348 (1972).

[9] M. Gavrila, Phys.Rev.A **6**, 1360 (1972).

[10] V. Florescu and M. Gavrila, Phys.Rev.A **14**, 211 (1976).

[11] (a) V.N. Litvinenko et al., Phys.Rev.Lett. **78**, 4569 (1997); (b) M. Hosaka et al., Nucl.Instr.and Meth.A **393**, 525 (1997); (c) M.E. Couprie et al., J.Phys.B **32**, 5657 (1999).

[12] V. Schönfelder (Ed.), *The Universe in Gamma Rays* (Springer, 2001).

[13] Z. Kaliman, T. Suric, K. Pisk, and R.H. Pratt, Phys. Rev. A **57**, 2683 (1998).

[14] A.I. Akhieser and V.B. Berestetskii, *Quantum Electrodynamics*, second edition (Interscience Publishers, Wiley, New York, 1965).

[15] A. Sommerfeld, *Atombau und Spektrallinien*, vol II (Vieweg, Braunschweig, 1939), Chap.VIII.

[16] J. Schwinger, J. Math. Phys.**5**, 1606 (1964).

[17] L. Hostler, J.Math.Phys. **5**, 591 (1964).

[18] L. Hostler, J.Math.Phys. **5** , 1235 (1964).

[19] M. Gavrila and A.Costescu, Phys.Rev.A **2**, 1752 (1970); **4**, 1688 (1971).

[20] See A. Erdelyi et al, *Higher Transcendental Functions* (McGraw and Hill, New York, 1953), vol. I.